VOL. 19, NO. 3, 2020, 35-48
www.elektrika.utm.my
ISSN 0128-4428

ELEKTRIKA
Journal of Electrical Engineering

A Quasi-Moment-Method-Based Calibration of Basic Pathloss Models

Ike Mowete*, **Michael Adedosu Adelabu**, **Ayotunde Abimbola Ayorinde**, **Hisham Abubakar Muhammed**, and **Francis Olutinji Okewole**

Department of Electrical and Electronics Engineering, University of Lagos, Akoka, Lagos, Nigeria.

*Corresponding author: amowete@unilag.edu.ng

Abstract: Using a technique similar to Harrington's method of moments, this paper develops a very simple but remarkably efficient approach to the calibration of established (basic) mobile radio propagation pathloss models. First, the theoretical foundations of the process, here referred to as the 'Quasi-Moment-Method (QMM)', is succinctly presented. Thereafter, for validation purposes, pathloss predictions due to its use are compared with corresponding data reported in the open literature, for a model that derived from the application of the Adaptive Neuro-Fuzzy Inference System, ANFIS. Results of the comparisons reveal that the root-mean square error (RMSE) values for the QMM-models compare favorably with those reported for the more computationally involved ANFIS model; and that all the six QMM-calibrated models considered in the paper, provided better spread-correlated root-mean-square (SC-RMS) and standard deviation (SD) prediction errors. QMM cross-application prediction performance is also evaluated through comparisons with measurement data obtained by the authors, for the Nigerian cities of Ibadan and Abuja. Outcomes of the comparisons clearly show that the QMM cross-application performance, particularly for the calibrated ECC-33 models, may be described as excellent.

Keywords: Pathloss model, Calibration, Moment-Method, Cross-application, ANFIS.

Article History: received 29 August 2020; accepted 6 December 2020; published 26 December 2020.

1. INTRODUCTION

In propagating from source to destination, electromagnetic waves are in varying degrees, invariably subjected to reflections, refractions, scattering, and absorption, with the consequence that signal degradation manifest as energy loss, conventionally referred to as 'pathloss', Ikegami and Yoshida, [1], Vieira et al., [2]: or channel propagation impairments, Sarkar et al. [3]. The radio link designer, in order to effectively plan, design, validate, and construct wireless communications networks, is consequently required to predict the nature and extent of signal quality degradation, and hence, account for the pathloss attributable to the system's operational environment. This need, in the case of mobile cellular communications, is particularly underscored by the requirements of Site Placement Problem (SPP) and Site Selection Problem (SSP), as described, respectively, in two different publications by Khalek et al., [4], and by Calegari et al., [5]; the latter concerning the Software Tools for the Optimisation of Resources in Mobile Systems (STORMS) project. Both publications represent notable examples of the critical importance of optimum pathloss models to the design and implementation of schemes for network performance optimization.

Although it is, in principle, possible to accurately specify terrain propagation loss characteristics by solving Maxwell's equations, subject to appropriate boundary conditions, this approach is decidedly mathematically rigorous and absolutely intractable in virtually all cases of practical interest, [3], [4]. A possible alternative is to utilize exhaustive measurements, which, in addition to being expensive, is clearly impractical. It is not surprising therefore, to find that researchers have, over the years, developed various methods and design tools in the form of empirical models Tutschku, [6]; Iskander and Yun, [7]; Fernandez et al., [8]; Gozalvez, Sepulcre and Palazon, [9], classified as either 'large-scale pathloss models' or 'small-scale fading models', with which to address these challenges. Unfortunately, it has been firmly established that it is impossible to find a model of such general applicability as to be independent of terrain, environmental conditions, and radio propagation scenario, [3]. Indeed, Erceg et al., [10], pointed out that classical pathloss models such as the Okumura-Hata [11] -and its derivatives-, rarely consider the needs of emerging communication systems and technology, and consequently inadequately provide for such needs, in network optimization schemes. Using a regression analysis approach, Erceg and his associates [10] analysed data available from comprehensive field measurements to obtain computational results, which suggest that this limitation may be addressed through the determination of optimum values for loss exponent and /or standard deviation of shadow fading indices, as may apply, in the model development process. One example that considered the needs of an emerging technology is offered by the contributions of Pitchaiah [12], whose work addressed the limitations imposed by the channel on the performance of the Local Multipoint Distribution Systems (LMDS) as a last mile solution in a wireless environment, utilizing the higher data rates. These contributions inform that pathloss prediction models are able to perform reliably, only to the extent that factors concerning the physical environment are suitably accounted for in the course of the model development process. This is the case with typical empirical modelling, in which data collection correctly reflects terrain and associated propagation characteristics.

Because the classical (basic) empirical models, despite the advantage of computational simplicity, often lack desirable levels of prediction accuracy, quite a few research efforts have been dedicated to 'tuning' or 'calibration' of the basic models, as a means of improving accuracy without losing ease of use. Notable examples of these optimization techniques include the contributions by Mardeni-Kwan[13], who implemented a regression-type 'Least Squares Method'; others are the regression analysis reported by Nissirat et al., [14], and the Genetic Algorithm optimization scheme, implemented by Garah and his associates, [15]. In the main, these approaches involve improving the Root Mean Square (RMS) prediction error due to such basic models as the Lee, [16], COST231-Hata [17], and COST231-Walfisch-Ikegami [18], and ECC-33 models, [19]. Although RMSE values as low as 3.08dB have been reported [15] as being due to the optimization of basic models with which RMSE values in excess of 20dB are otherwise associated, it is still held [20-22], that the associated prediction errors are in general, rather poor. As a consequence, research attention has been directed in recent times, to the development of empirical models, with basis in artificial intelligence techniques. These include the various Artificial Neural Networks (ANN)-based models described by Sotiroudis et al., [19], Cavalcanti and Cavalcante, [21], and Eichie et al., [22]. Others are the variants of the Adaptive Neuro-Fuzzy Inference Systems (ANFIS)-based methods reported by Larijani, Curtis, and Wistex, [23], and the contributions by Faruk and his associates, [24 25]; as well as the Support Vector methods due to Timoteo [26], and Zhao, [27], and the Learning Machine approach introduced by Ayadi et al., [28].

As pointed out by Faruk et al., [25], and Surajudeen-Bakinde et al. [33], whereas the ANN and ANFIS-based models outperform the basic models in terms of Mean Prediction Error (MPE) and RMSE as performance metrics, the basic (uncalibrated) models outperform the ANN/ANFIS models, when Standard Deviation Error (SDE) is utilized as performance metric. For this reason, [25] suggested that in practical situations a trade-off between simplicity and ease of use (due to optimized basic models) on one hand, and on the other, accuracy and computational complexity (attributed to the ANN/ANFIS models) should prove expedient. It was further suggested in [25] that a hybrid of these two approaches could be the best option. And indeed, this suggestion is very strongly supported by the results reported by Cavalcanti and Cavacante [21], who utilized a hybrid of ECC-33, Ericsson, and Tr-36.942 for pathloss prediction concerning LTE and LTE-A networks.

This paper presents a novel, a very simple, yet remarkably efficient approach to empirical pathloss calibration, which, on account of its similarity to the Matrix Methods originally developed by Harrington, [32], for the solution of field problems, is referred to as the 'Quasi-Moment-Method', or 'QMM'. For the purposes of validating the correctness and efficacy of the approach, pathloss predicted with its use is compared with measurement (and associated) data published in [24], and the outcomes of the comparison revealed that the model compares favourably with the more computationally intensive ANFIS model utilized in [24]. For example, in terms of MPE, respective values of -0.0289 and $9.85\text{x}10^{-6}$ were recorded for the best performing QMM-calibrated ECC-33 and ANFIS models; and in the case of RMSE, SC-RMSE, and SDE, values (in dB) obtained for the QMM-calibrated ECC-33 model are (4.9854, 3.7326, 1.9783**),** respectively, as against (2.5023, 4.4881, 6.0535**)** respectively, for ANFIS as published in [24].

2. THEORETICAL BACKGROUND

The generic pathloss empirical model is conceived in this paper, as a solution to the 'approximation problem', as defined by Dahlquist and Bjorck, [31]. Accordingly, we let $P_l(d)$ represent the continuous function, which accurately specifies propagation pathloss for the region of interest, and which is to be approximated by the function

$$P_l^*(d) = \alpha_1\varphi_1(d) + \alpha_2\varphi_2(d) + \mathrm{K} + \alpha_N\varphi_N(d), \quad (1)$$

in which the set $\{\varphi_k\}$ represents a set of known functions, and $\{\alpha_k\}$, a set of unknown coefficients to be determined. The solution to this 'approximation problem' is considered optimum, when the unknown coefficients are so specified that the (weighted) Euclidean semi-norm of the error function defined as

$$\varepsilon = P_l^*(d) - P_l(d), \quad (2)$$

assumes its minimum possible value, for all values of the independent variable 'd'. That is,

$$\left\| P_l^*(d) - P_l(d) \right\|^2 \equiv \sum_{k=1}^{N} \left| P_l^*(d_k) - P_l(d_k) \right|^2 \quad (3)$$

is as small as possible.

As shown in [31], when $\{\varphi_k\}$ is set of linearly independent functions, the solution to the approximation problem emerges as

$$P_l^*(d) = \sum_{n=1}^{N} \alpha_n\varphi_n(d), \quad (4)$$

provided that the unknown coefficients are solutions to the 'normal equation', given as

$$\begin{aligned}
&\langle\varphi_1,\varphi_1\rangle\alpha_1+\langle\varphi_1,\varphi_2\rangle\alpha_2+\langle\varphi_1,\varphi_3\rangle\alpha_3+\text{K}+\langle\varphi_1,\varphi_N\rangle\alpha_N=\langle\varphi_1,P_l\rangle \\
&\langle\varphi_2,\varphi_1\rangle\alpha_1+\langle\varphi_2,\varphi_2\rangle\alpha_2+\langle\varphi_2,\varphi_3\rangle\alpha_3+\text{K}+\langle\varphi_2,\varphi_N\rangle\alpha_N=\langle\varphi_2,P_l\rangle \\
&\quad . \\
&\quad . \\
&\langle\varphi_N,\varphi_1\rangle\alpha_1+\langle\varphi_N,\varphi_2\rangle\alpha_2+\langle\varphi_N,\varphi_3\rangle\alpha_3+\text{K}+\langle\varphi_N,\varphi_N\rangle\alpha_N=\langle\varphi_N,P_l\rangle
\end{aligned} \tag{5}$$

The inner product terms appearing in Eqn. (5) admit description, according to, [31],

$$\begin{aligned}
\langle\varphi_m,\varphi_n\rangle &\equiv \sum_{k=1}^{K}\varphi_m(d_k)\varphi_n(d_k) \\
\langle\varphi_m,P_l\rangle &\equiv \sum_{k=1}^{K}\varphi_m(d_k)P_l(d_k)
\end{aligned} \tag{6}$$

Equation (5) can be cast in matrix format, if the following definitions are utilized:

$$[\Phi]\equiv\begin{bmatrix} \langle\varphi_1,\varphi_1\rangle & \langle\varphi_1,\varphi_2\rangle & \cdots & \langle\varphi_1,\varphi_N\rangle \\ \langle\varphi_2,\varphi_1\rangle & \langle\varphi_2,\varphi_2\rangle & \cdots & \langle\varphi_2,\varphi_N\rangle \\ \cdots & \cdots & \cdots & \cdots \\ \langle\varphi_N,\varphi_1\rangle & \langle\varphi_N,\varphi_2\rangle & \cdots & \langle\varphi_N,\varphi_N\rangle \end{bmatrix}, \tag{7a}$$

$$\lfloor\Pi\rfloor=\begin{bmatrix} \langle\varphi_1,P_l\rangle \\ . \\ . \\ \langle\varphi_N,P_l\rangle \end{bmatrix}, \tag{7b}$$

and

$$[\Upsilon]=\begin{bmatrix} \alpha_1 \\ \alpha_2 \\ . \\ . \\ \alpha_N \end{bmatrix}, \tag{7c}$$

so that the desired unknown coefficients are obtained through the simple matrix operations of inversion and multiplication as

$$[\Upsilon]=[\Phi]^{-1}[\Pi] \tag{8}$$

Equation (8) is similar to matrix equation for the moment-method, expressed in terms of generalized network parameters, [32].

Six of the more common basic pathloss models, namely, the Okumura-Hata, COST231-Hata, ECC-33, Egli, Ericsson, and Lee models, were selected as 'base' or 'reference' models, for the implementation of the QMM scheme described in the foregoing. In the case of the Okumura-Hata model, as illustrative example, the 'base' model is given, for urban centers, as, [13],

$$\begin{aligned}
P_l(Urban) &= 69.55+26.16\log_{10}(f)-13.82\log_{10}(h_{te})-a(h_{re}) \\
&+\left(44.9-6.55\log_{10}(h_{te})\right)\log_{10}(d)
\end{aligned} \tag{9a}$$

In Eqn. (9a), h_{te} represents effective transmitter height, and h_{re} stands for effective mobile receiver antenna height, both measured in meters. The parameter $a(h_{re})$ is a correction factor for effective mobile antenna height, and is given, for small-to-medium sized cities as

$$a(h_{re})=\left(1.1\log_{10}(f)-0.7\right)h_{re}-\left(1.56\log_{10}(f)-0.8\right) \tag{9b}$$

and for large cities,

$$a(h_{re})=8.29\left(\left(\log_{10}(1.55h_{re})\right)^2\right)-1.1, \quad f\le 300MHz \tag{9c}$$

or

$$a(h_{re})=3.2\left(\left(\log_{10}(11.75h_{re})\right)^2\right)-4.97, \quad f\ge 300MHz \tag{9d}$$

For the sub-urban environment, Eqn. (9a) modifies to

$$P_l(sub-urban)=P_l(urban)-2\left(\log_{10}\left(f/28\right)\right)^2-5.4 \tag{10}$$

Thus, in utilizing this 'base' model for the solution to the approximation problem of interest to the optimum model calibration process under discussion here, the following identification is made for the set $\{\varphi_k\}$:

$$\begin{Bmatrix}\varphi_1\\\varphi_2\\\varphi_3\\\varphi_4\\\varphi_5\end{Bmatrix}\equiv\begin{Bmatrix} 69.55 \\ 26.16\log_{10}(f) \\ -13.82\log_{10}(h_{te}) \\ -a(h_{re}) \\ \left(44.9-6.55\log_{10}(h_{te})\right)\log_{10}(d) \end{Bmatrix} \tag{11}$$

Since the $\{P_l(d_k)\}$ are available from the processed field measurements, the only unknown quantities are the $\{\alpha_k\}$, which are readily determined from the matrix operations of inversion and multiplication.

2.1 Model Performance Evaluation and Validation

For the purposes of ascertaining the validity and efficacy of the formulation, prediction results due to QMM-calibrated basic models are compared with corresponding measurement results reported in [24], and with which the calibration of the basic models was effected. In addition, the performances of the various QMM-modified models are compared, in terms of MPE, RMSE, SC-RMSE, and SDE, with the performance of an ANFIS model, as reported in [24], for the same sets of measurement data.

Outcomes of this evaluation are displayed in the graphical formats of Fig. (1) and Fig. (2), as well as the statistical performance metrics shown in Table 1.

It is apparent from both Figs. (1) and (2) that the six QMM-calibrated reference models performed well-within the error bounds established by Phillips et al. [34]. This observation is supported by the associated computational results displayed in Table 1, concerning the statistical performance metrics of RMSE, SC-RMSE, MPE, and SDE, for the ANFIS and corresponding QMM-calibrated models. These results reveal that whereas the ANFIS model recorded better RMSE and MPE metrics than the QMM-modified models, the latter models, in all cases, had better SC-RMSE and SDE metrics than the former. It should be remarked that even where the much more computationally intensive ANFIS model had better metrics, the corresponding metrics for the computationally inexpensive QMM models were comparable. And this observation is consistent with the remark in [25] that choice of use between ANFIS and efficiently calibrated

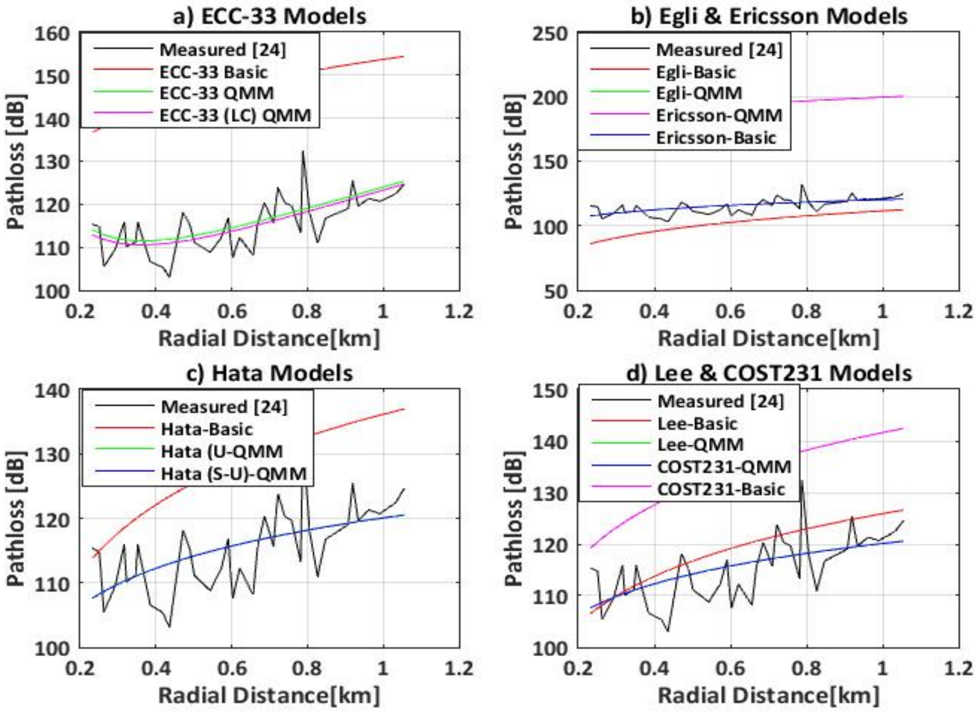

Figure 1. Comparison of prediction of QMM-models with measurement data from Fig 7 [24].

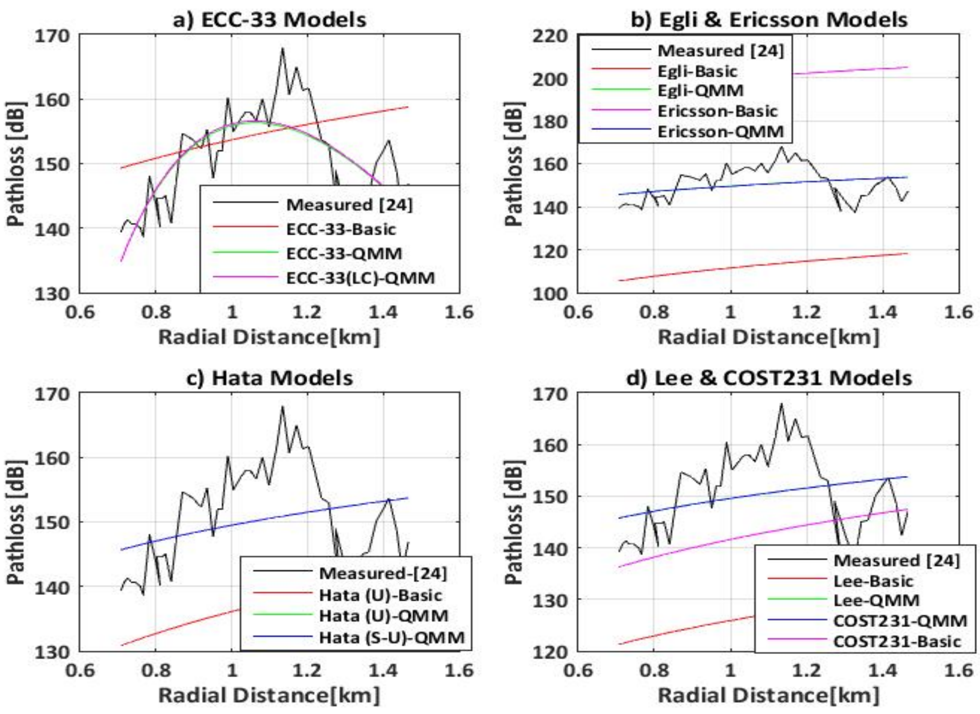

Figure 2. Comparison of prediction of QMM-models with measurement data from Fig 8 [24].

Table 1. Comparative performance evaluation of QMM-Models

	Figure 7 [24]				**Figure 8 [24]**			
MODEL/ METRIC	**RMSE (dB)**	**SC- RMSE (dB)**	**MPE (dB)**	**SDE (dB)**	**RMSE (dB)**	**SC- RMSE (dB)**	**MPE (dB)**	**SDE (dB)**
ANFIS [24]	2.5023	4.4881	9.85E-06	6.0535	1.5378	6.9608	4.98E-05	7.8850
COST231-QMM	4.9854	3.9115	-0.0298	2.5816	7.5309	4.1702	-0.0097	5.5325
ECC-33-QMM	4.6105	3.7326	-0.8514	1.9781	5.1898	5.1559	0.0260	1.9911
ECC-33(LC)-QMM	4.5312	3.8729	-0.0266	1.9714	5.1924	5.1777	-0.1639	1.9177
EGLI-QMM	4.9853	3.9105	-0.0066	2.5814	7.5309	4.1722	-0.0090	5.5328
ERICSSON-QMM	4.9860	3.97.53	-0.0858	2.5816	7.5321	4.1776	0.0532	5.5365
HATA-URB-QMM	4.9853	3.9112	-0.0234	2.5820	7.5310	4.1762	0.0428	5.5325
HATA(SUB)-QMM	4.9853	3.9085	0.0168	2.5822	7.5310	4.1759	0.0401	5.5329
LEE-QMM	4.9858	3.9137	-0.0724	2.5812	7.5310	4.1703	-0.0505	5.5327

basic models will depend on a trade-off between prediction accuracy and ease of model implementation.

With the validation, through the foregoing comparative analysis, of the QMM-calibration technique, its use with the calibration of basic models, using measurement results obtained for the Nigerian cities of Abuja and Ibadan as candidates, will be addressed in the ensuing sections.

3. MEASUREMENT CAMPAIGNS

Quite a few of the previously existing empirical models described in the open literature, [13, 14], have their bases in ‘optimization schemes’ designed to better fit basic models to measurement data for signal strength or power density collected for the terrain of interest. In the typical case, exemplified by the two references just cited, averages are taken, of measurements obtained from several base stations, and utilized as representative of the city for which a pathloss profile is to be established. A slight variation of this approach is adopted in this paper. Measurements taken for individual base stations are averaged for contiguous geographical locations, and this average is taken as representative of the geographical area covered by the base stations.

3.1 Data Collection

Two candidate Nigerian cities, Ibadan and Abuja, were considered for this paper, and the model calibration process was preceded by a phase of extensive data collection. Data sets were sourced from official measurement data on the existing networks of two major services providers in Nigeria, namely, MTN [29] and Airtel, [30]. In addition, field measurements were taken from 2009-2011 and later 2012-2013 at different times to cover the various seasons – wet rainy, and dry harmattan seasons. The measurements were informed by the distribution of the base stations across the locations, as made available by the services providers, and representative examples of which are displayed in Tables 2 (for Abuja) and Table 3 (for Ibadan).

Comprehensive data sets made available by the service providers included results of drive tests conducted on the two networks between 2007 and 2012, courtesy of engineering staff of the networks. Test equipment utilized for the field work include Lenovo ThinkPad and Toshiba Equium laptops, TEMS compatible mobile station – Sony Ericsson C702, USB GPS instrument, and TEMS dongle for real time drive-test data capture. A series of measurements were taken with SA2650 handheld spectrum analyzer having the frequency range 100kHz to 3.5GHz, and Carmin handheld GPS instrument were used as control data to verify the drive test results. Data capture and processing were carried out with the Toshiba laptop.

4. COMPUTATIONAL RESULTS AND DISCUSSIONS

For all computational results presented here, base station antenna height is 30m, and mobile station antenna height is 1.5m. All the base stations operated within the GSM-1800MHz frequency band.

4.1 Pathloss Prediction by the QMM-models for Abuja

Results presented in graphical formats in this section, concern the seven base stations, for which average pathloss, as earlier described, were obtained. The pathloss profiles in figure 3 refer to measured pathloss values obtained for BTS1, BTS2, BTS3, and BTS4 of Abuja, as identified in Table 2. And it is apparent from the profiles, that the best fit is due to the ECC-33 (QMM) models. Indeed, as can be seen from Table 4, the ECC-33 models (but for two exceptions) have the best performing statistical indices. The exceptions to this observation are in the cases of Mean Prediction Error (MPE) for the QMM-calibrated Lee model, which performed better; as well as Spread-Correlated RMSE (SC-RMSE), for which the QMM-modified Hata (Sub-Urban) model had the best index of 5.3397dB. As a matter of fact, in terms of RMSE, the QMM-calibrated Lee model consistently came third, next to the ECC-33 and ECC-33 (Large City) models, in that order. One other remarkable feature of the results is that the Basic-COST231 model had a MPE (-1.4036dB) almost the same in magnitude (-1.3296dB) as its QMM-

VOL. 19, NO. 3, 2020, 35-48
www.elektrika.utm.my
ISSN 0128-4428

Table 2. Examples of the Abuja Cell Sites utilized in this study Source [30]

New site ID	TAG	City/District	Capacity Dimension Area	Longitude	Latitude	BSC
AB0009	BTS1	Garki	Abuja Metropolis	7.47268	9.01526	EABBS02
AB0043	BTS2	Garki	Abuja Metropolis	7.4930537	9.0323886	EABBS01
AB0061	BTS3	Garki	Abuja Metropolis	7.4841082	9.037777	EABBS01
AB0063	BTS4	Garki II	Abuja Metropolis	7.497663	9.0395236	EABBS01
AB0006	BTS5	Garki II	Abuja Metropolis	7.48801	9.08198	EABBS01
AB0018	BTS6	Maitama	Abuja Metropolis	7.48091	9.10639	EABBS02
AB0019	BTS7	Maitama	Abuja Metropolis	7.50487	9.09258	EABBS01

Table 3. Examples of the Ibadan Cell Sites Utilized in this study Source [30]

New site ID	TAG	City/District	Capacity Dimension Area	Longitude	Latitude	BSC
OY0041	BTS1	Ibadan	Ibadan	3.8535035	7.3429193	EOYBS01
OY0030	BTS2	Ibadan	Ibadan	3.8536683	7.3794129	EOYBS01
OY0058	BTS3	Ibadan	Ibadan	3.8700244	7.3385585	EOYBS01

calibrated version; though the latter recorded much better performances with the other indices.

Similar trends are displayed in the cases of BTS' 2, 3, and 4, as can be seen from Figs. (4)-(6), and Table 4. The last column of Table 4 displays the statistical performance metrics of QMM models, calibrated with the use of pathloss, averaged over seven BTS', at each radial distance away from the transmitting antenna. These results suggest that when average values, taken over a large data set are utilized for QMM pathloss calibration, performance improves remarkably.

As an example, for the best performing ECC-33 model, RMSE improved from the worst recorded case of 2.8505dB, for BTS1, to 0.4452dB, in the case of pathloss average. It is also readily observed that RMSE performances improved to below 5.0 dB for all the other models, except for the worst performing Hata (sub-urban) model, for which RMSE, nonetheless, improved from 11.5998 (for BTS2) to 7.8784dB. It may be concluded that this Hata (sub-urban) model is clearly a poor reference model, for use with pathloss model calibration for Abuja.

4.1.1. Cross-Application performances of the QMM Pathloss Models -Abuja

In a recent publication, Zhang et al., [35], introduced '*cross-application*' as a performance metric, defined as a measure of the ability of a basic model calibrated with measurements in a given area, to accurately predict pathloss in some other area with similar terrain features. A variation of that definition is adopted in this paper. 'Cross-application' is taken here, as referring to the ability of a QMM-model, calibrated with pathloss averaged over a set of BTS', to accurately predict pathloss for individual BTS' within the set. Two different scenarios, based on this adaptation of the term, are examined in this section. The first involves BTS' 1 to 5 (Garki), and the second, BTS' 6 and 7, for Maitama. The pathloss profiles of Figs. (7) and (8), for BTS' 1 to 5, and BTS' 6 and 7, respectively, compare pathloss predicted on the basis of calibration with 'BTS' group averages' on one hand, with measured pathloss for some BTS' in the group, on the other.

In the case of the profiles of Fig. (7) and the corresponding statistical performance metrics displayed in Table 5, it is readily observed that the ECC-33 calibrated models are able to predict individual BTS pathloss with RMSE values ranging between 2.8973dB for BTS4, and 5.533dB for BTS3. All other models (with the exception of the sub-urban Hata model), in most of the cases, also performed creditably well in this regard.

The same general trend is repeated for the group including BTS' 6 and 7, whose pathloss profiles are displayed in Fig. (8). In this case though, a different pattern of RMSE values emerged. For example, in the case of BTS 6, the best 'cross-application' performing QMM-calibrated model is the Egli model (3.0860dB) and the worst performing is the Ericsson model, for which a value of 4.8269dB was recorded, for RMSE.

Another interesting feature in the case of BTS 6, is that both the QMM-calibrated Egli and Hata (urban area) models, in that order, recorded better RMSE (3.0860dB; 3.3591dB) values than the ECC-33 calibrated models. And indeed, both models (Egli and Hata (urban)), again, in the same order, had better cross-application MPE values than the ECC-33 models.

4.2 Cross-Application performances of the QMM Pathloss Models -Ibadan

As a second example of the cross-application performances of the six QMM-calibrated models considered in this paper, the case of predicted pathloss profiles obtained from models calibrated with some measurements taken in Ibadan is presented in this section.

First, the performances of six calibrated models are compared with the measurement data from which they derive. The pathloss profiles of Fig. (9) graphically describe these performances, in the case of BTS2 of Table 3, as an example.

Computational results concerning statistical performance metrics for these cases further describe the performances of the calibrated models. For example, in the case of Fig. 9(a), 1.9872dB was recorded as RMSE for the two QMM-ECC-33 models, and for Fig. 9 (b), RMSE values of 7.2131dB and 7.5865dB were recorded, respectively, for the calibrated Ericsson and Egli models. For BTS' 1 and 3, the ECC-33 models still give the best performances, though results for BTS 2, for the models represent the best.

Using the definition adopted in this paper for 'cross-application', the performances of the calibrated models for the three BTS' considered for Ibadan, are described by the profiles of Fig. (10). The 'QMM-models' in the illustrations refer to the basic models, calibrated in this case, with average pathloss, taken over the three BTS' listed for Ibadan.

As was the case for the two Abuja scenarios earlier described, the best performing 'cross-application' models for Ibadan are the ECC-33 models (RMSE(dB) = 3.0295; 2.3187; 5.1182; for BTS' 1, 2, and 3, respectively), but a number of interesting departures occur in this case. For BTS1, the COST231 recorded the next best RMSE value of 5.8926dB, but for BTS' 2 and 3, it was the calibrated Hata (urban-5.9536dB) and Ericsson (5.1128dB) models, respectively, that came after the ECC-33 models. In terms of MPE, the Lee models generally performed best, though corresponding values for the ECC-33 models were quite close. On the other hand, the ECC-33 models recorded far better Mean Absolute Error (MAE) results.

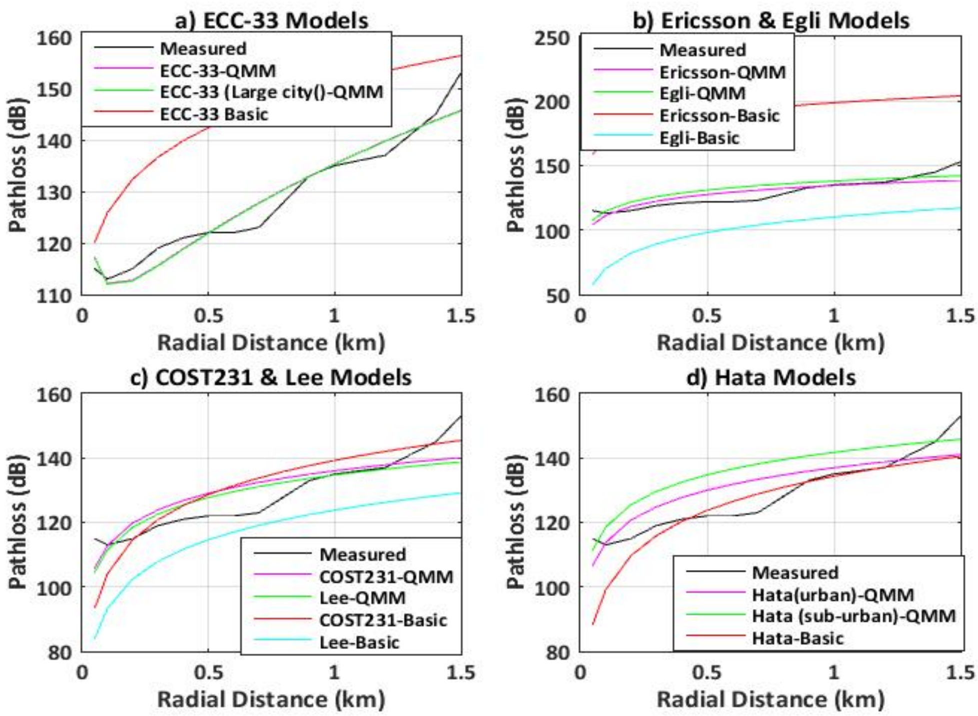

Figure 3. Predicted pathloss profiles for BTS 1 of Abuja

Table 4. Statistical performance metrics for the QMM models: Abuja

Model/BTS	BTS1 (dB)	BTS 2 (dB)	BTS 3 (dB)	BTS 4 (dB)	Average (dB)
COST231	MPE =-1.3286 RMSE =6.2475 MAE = 5.0985 SDE = 1.7333	MPE =-1.3217 RMSE =9.3105 MAE = 8.0922 SDE = 3.1027	MPE =-1.2861 RMSE =4.7547 MAE = 5.5333 SDE = 0.6526	MPE =-1.3769 RMSE =2.5934 MAE = 2.2135 SDE = 0.1375	MPE =-1.2747 RMSE =4.2086 MAE = 3.4565 SDE = 0.7605
ECC-33 (LC)	MPE =0.0777 RMSE =2.8411 MAE = 2.1852 SDE = 0.3848	MPE =0.0772 RMSE =2.0391 MAE = 1.6109 SDE = 0.6108	MPE =0.0672 RMSE =2.1408 MAE = 1.7254 SDE = 0.1684	MPE =0.0763 RMSE =1.5242 MAE = 1.2074 SDE = 0.1256	MPE =0.0732 RMSE =0.4496 MAE = 0.3344 SDE = 0.0249
ECC-33	MPE =-0.0368 RMSE =2.8405 MAE = 2.1820 SDE = 0.4026	MPE =--0.0234 RMSE =2.0290 MAE = 1.6306 SDE = 0.1775	MPE =-0.0186 RMSE =2.1396 MAE = 1.7329 SDE = 0.1869	MPE =-0.0207 RMSE =1.5228 MAE = 1.1862 SDE = 0.1456	MPE =-0.0208 RMSE = 0.4452 MAE = 0.3438 SDE = 0.0420
EGLI	MPE =-3.3011 RMSE =6.9400 MAE = 6.0624 SDE = 1.2601	MPE =-2.3902 RMSE =9.6698 MAE = 8.1576 SDE = 2.8208	MPE =-5.2400 RMSE =6.9601 MAE = 6.0908 SDE = -0.2789	MPE =-3.0358 RMSE =3.7492 MAE = 3.0486 SDE = -0.2019	MPE =-2.8303 RMSE =4.9090 MAE = 4.1615 SDE = 0.4186
ERICSSON	MPE =0.1727 RMSE =6.1607 MAE = 4.1740 SDE = 1.8269	MPE =0.1515 RMSE =9.2164 MAE = 8.0493 SDE = 3.1703	MPE =-0.1492 RMSE= 4.5830 MAE = 3.1750 SDE = 0.7109	MPE =0.1558 RMSE =2.2053 MAE = 2.0238 SDE = 0.2264	MPE =0.1497 RMSE =4.0137 MAE = 3.3242 SDE = 0.8494
HATA -SUB	MPE =-7.0361 RMSE =9.3152 MAE = 8.3663 SDE = -0.5413	MPE =-7.0452 RMSE =11.5998 MAE = 9.4161 SDE = 0.2364	MPE =-6.8156 RMSE =8.2417 MAE = 7.4801 SDE = -0.8357	MPE =-7.2945 RMSE =7.6141 MAE = 2.2943 SDE = 2.0609	MPE =-6.7809 RMSE =7.8784 MAE = 7.0576 SDE = -1.4192
HATA(URBAN)	MPE =-2.2595 RMSE =6.5093 MAE = 5.5416 SDE = 1.5576	MPE =-2.2702 RMSE =9.4904 MAE = 8.0921 SDE = 2.9613	MPE =-2.2010 RMSE =5.0819 MAE = 4.1049 SDE = 1.5443	MPE =-2.3467 RMSE = 3.2167 MAE = 2.7315 SDE = -0.0300	MPE =-2.1784 RMSE =4.5643 MAE = 3.8622 SDE = 0.5904
LEE	MPE =-0.0092 RMSE =6.1604 MAE = 4.7408 SDE = 1,8266	MPE =-0.0144 RMSE =9.2152 MAE = 8.0921 SDE = 3.1766	MPE =-0.0174 RMSE =4.5806 MAE = 3.1485 SDE = 0.7106	MPE =-0.0056 RMSE =2.2000 MAE = 2.0431 SDE = 0.2269	MPE =-0.0150 RMSE =4.0170 MAE = 3.3241 SDE = 0.8493

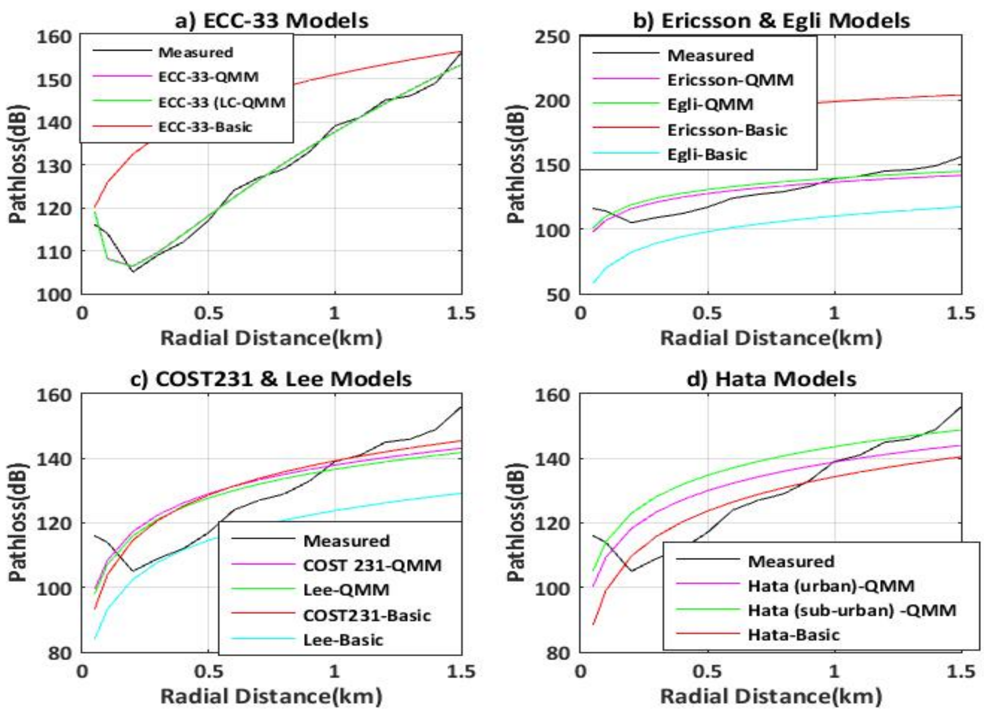

Figure 4. Predicted pathloss profiles for BTS2 of Abuja

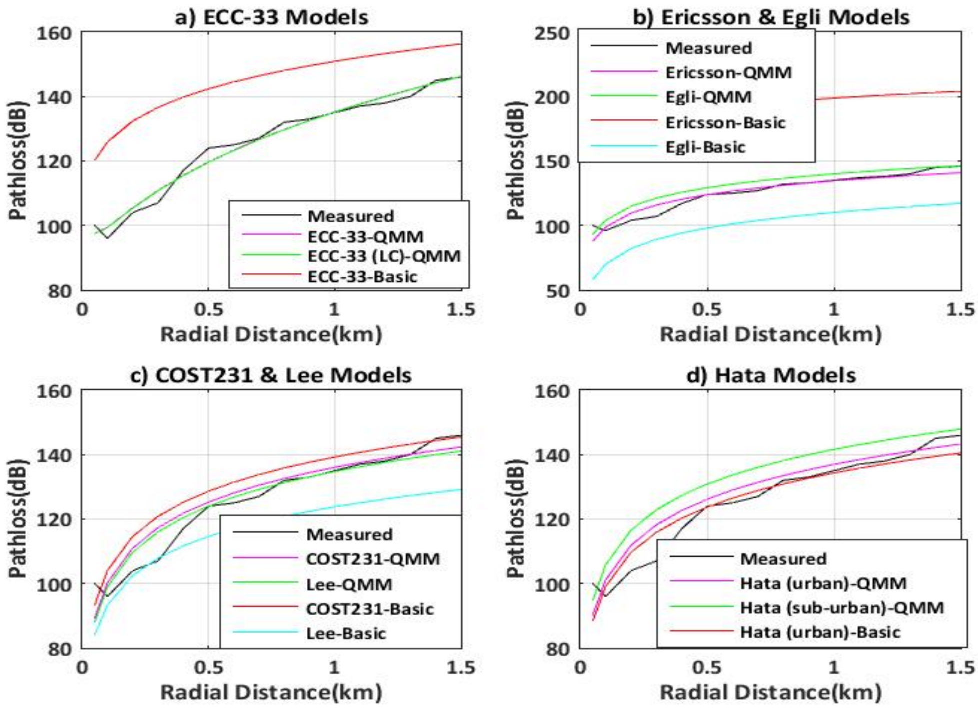

Figure 5. Predicted pathloss profiles for BTS 3 of Abuja

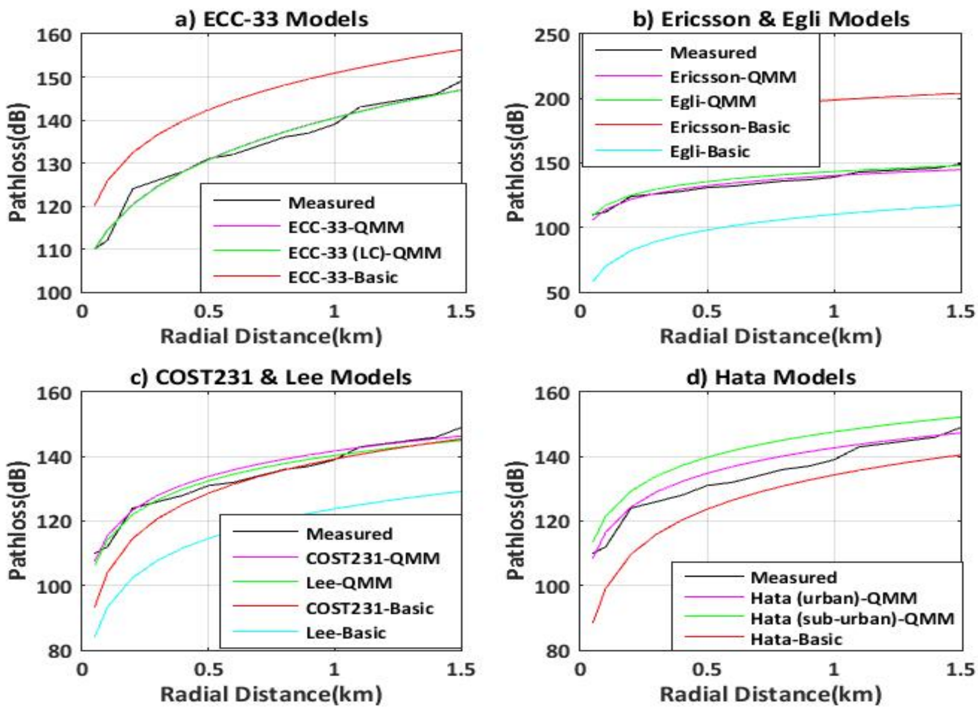

Figure 6. Predicted pathloss profiles for BTS 4 of Abuja

VOL. 19, NO. 3, 2020, 35-48
www.elektrika.utm.my
ISSN 0128-4428

ELEKTRIKA
Journal of Electrical Engineering

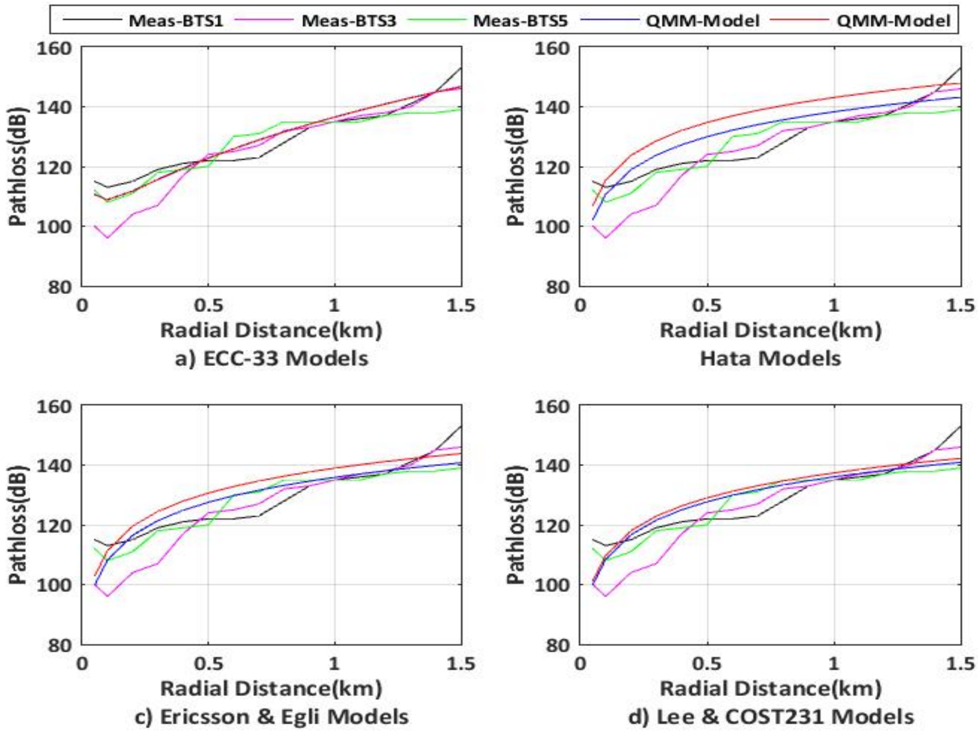

Figure 7. Cross-application pathloss profiles: QMM-predicted Vs. BTS' 1, 3, and 5 of Abuja

Table 5. Statistical Cross-Application performance metrics for the Abuja QMM-models

Model/Cluster	BTS1 (dB)	BTS 2 (dB)	BTS 3 (dB)	BTS4 (dB)	BTS5 (dB)
COST231	MPE =1.4953 RMSE =6.5575 MAE = 5.5743 SDE = 0.2047	MPE =1.3453 RMSE =9.3288 MAE = 8.1702 SDE = 3.8784	MPE =-4.7453 RMSE =7.4133 MAE = 5.6636 SDE = 2.2366	MPE =3.3797 RMSE =4.0801 MAE = 3.3797 SDE = -0.9150	MPE =-2.5678 RMSE =4.9052 MAE = 3.9318 SDE = -1.2348
ECC-33 (LC)	MPE =0.0845 RMSE =3.4905 MAE = 6.2312 SDE = 0.5258	MPE =0.1656 RMSE =4.4270 MAE = 4.3056 SDE = 3.0558	MPE =-3.3345 RMSE =5.487 MAE = 3.5732 SDE = 2.8660	MPE =4.7906 RMSE =5.8819 MAE = 4.8539 SDE = -2.2281	MPE =-1.1470 RMSE =3.6386 MAE = 2.9719 SDE = -1.8942
ECC-33	MPE =0.1827 RMSE =3.4839 MAE = 3.0434 SDE = 0.9873	MPE =0.0673 RMSE =4.9276 MAE = 4.3676 SDE = 3.0755	MPE =3.4327 RMSE =5.3243 MAE = 5.6378 SDE = 2.8514	MPE =4.6923 RMSE =5.8007 MAE =4.7841 SDE = -0.9150	MPE =-1.2452 RMSE =3.6621 MAE = 2.9919 SDE = -1.8553
EGLI	MPE =3.0948 RMSE =7.0950 MAE = 6.2038 SDE =0 .05258	MPE =2.8448 RMSE =9.2487 MAE =8.1703 SDE = 3.5912	MPE =-6.3448 RMSE =8.5266 MAE = 6.8635 SDE = 2.5220	MPE =1.7802 RMSE =2.8970 MAE = 2.0882 SDE = -0.5538	MPE =-4.5178 RMSE =5.8991 MAE = 5.2911 SDE = -1.6988
ERICSSON	MPE =0.0072 RMSE =6.3842 MAE = 4.9100 SDE = 0.1032	MPE =0.2428 RMSE =9.2487 MAE = 8.1704 SDE = 3.9488	MPE =-3.2572 RMSE =6.3620 MAE = 4.6886 SDE = 3.7414	MPE =4.8678 RMSE =5.3776 MAE = 4.8678 SDE = -1.4306	MPE =-1.0699 RMSE =4.3915 MAE = 2.8979 SDE = -0.9987
HATA -SUB	MPE =7.2032 RMSE =9.6256 MAE = 8.0301 SDE = 2.2309	MPE =6.9532 RMSE =11.5682 MAE = 9.3151 SDE = 1.9480	MPE =-10.4532 RMSE =8.0225 MAE = 10.4532 SDE = 0.0379	MPE =-2.2382 RMSE =3.2628 MAE = 2.8601 SDE = -0.6543	MPE =-8.2657 RMSE =9.2651 MAE = 8.8833 SDE = -3.6949
HATA(URBAN)	MPE =2.4259 RMSE =6.8301 MAE = 5.8796 SDE = 0.3659	MPE =2.1759 RMSE =9.4979 MAE = 8.1702 SDE = 3.7373	MPE =8.0408 RMSE =6.3615 MAE = 2.8406 SDE = 5.6759	MPE =2.4491 RMSE =3.3501 MAE =2.4719 SDE = 0.6978	MPE =-3.4884 RMSE =5.4487 MAE = 4.7061 SDE = -1.4822
LEE	MPE =0.1707 RMSE =6.3868 MAE = 4.9775 SDE = 0.1057	MPE =0.0743 RMSE =9.2457 MAE = 8.1703 SDE = 3.9486	MPE =-3.4207 RMSE =6.6441 MAE = 4.7709 SDE = 3.69365	MPE =4.4703 RMSE =5.2302 MAE = 4.7403 SDE = -1.3668	MPE =-1.2332 RMSE =4.3633 MAE = 2.9898 SDE = -1.0161

VOL. 19, NO. 3, 2020, 35-48
www.elektrika.utm.my
ISSN 0128-4428

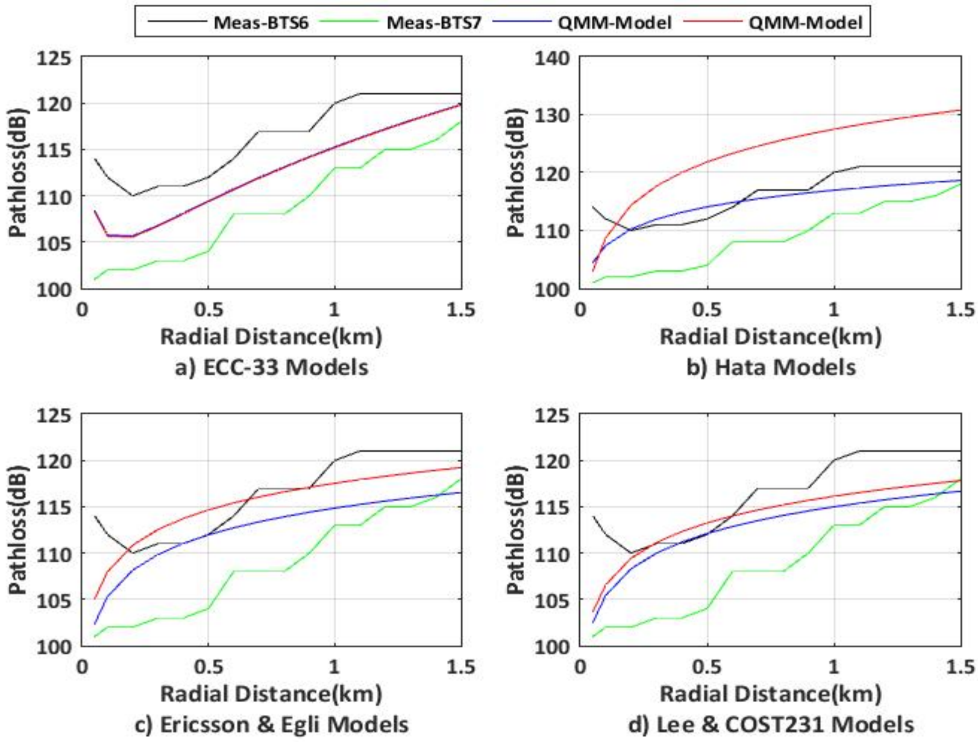

Figure 8. Cross-application pathloss profiles: QMM-predicted Vs. BTS' 6, and 7- Abuja

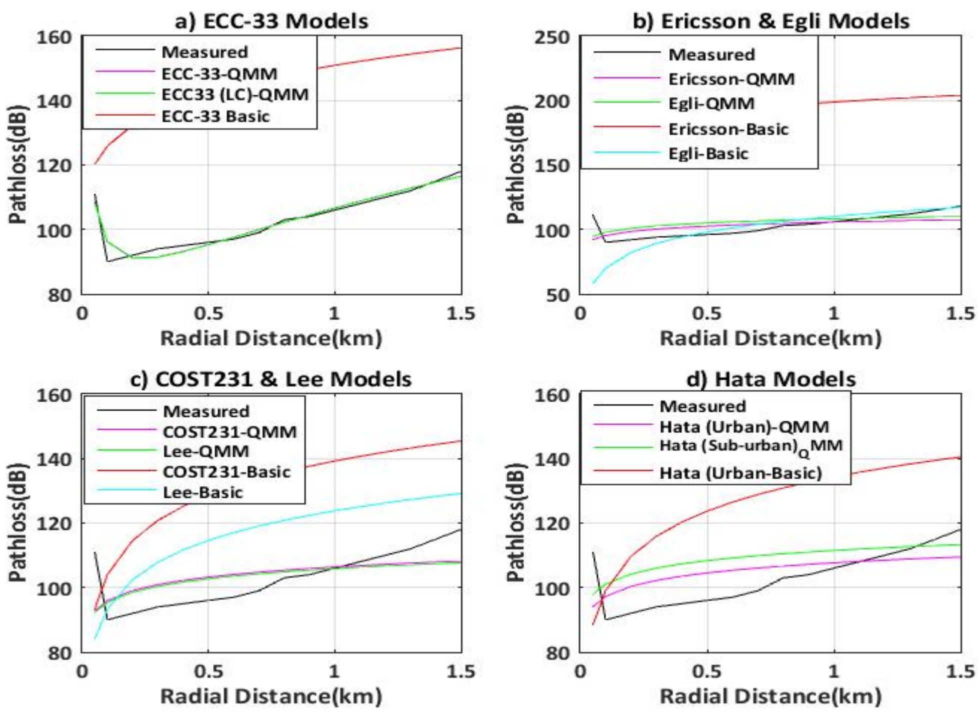

Figure 9. Comparison of pathloss profiles: QMM-predicted Vs. Measured BTS2- Ibadan

ELEKTRIKA
Journal of Electrical Engineering

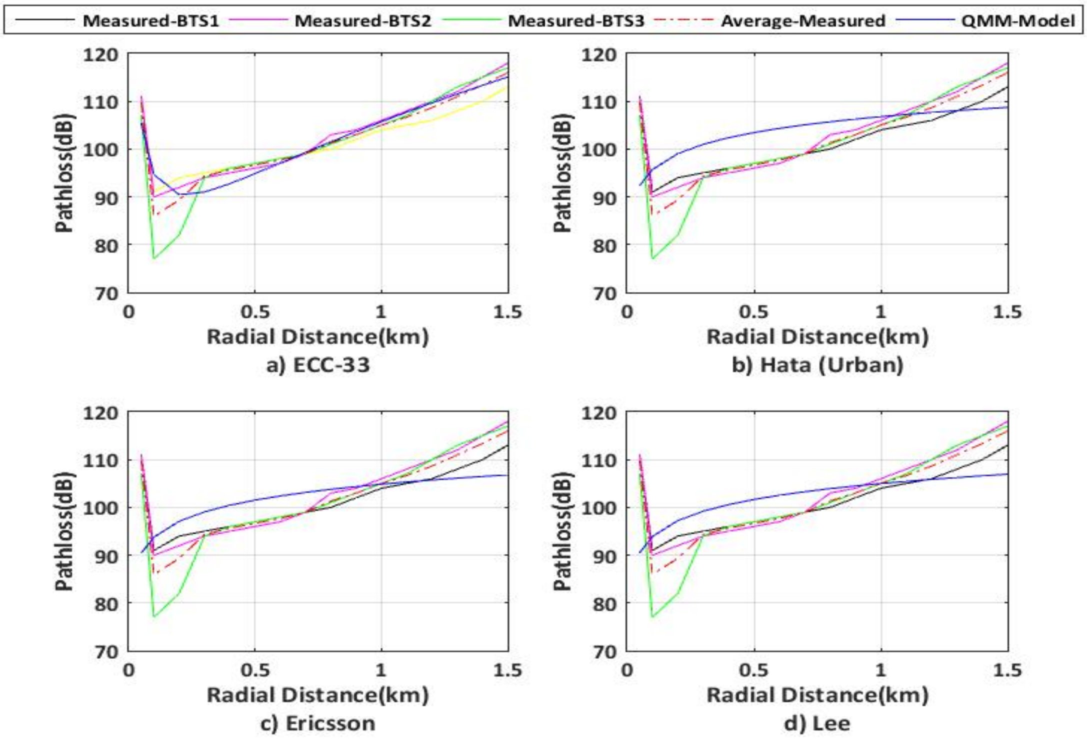

Figure 10. Cross-application pathloss profiles: QMM-predicted Vs. BTS' 1, 2, and 3- Ibadan

5. CONCLUDING REMARKS

This paper has presented the 'Quasi-Moment-Method' (QMM) as a very simple and remarkably efficient calibration tool for empirical radio propagation pathloss modeling. After a succinct description of the method's characterizing features, predictions due to its use were compared with corresponding predictions published in [24], in which the ANFIS method was utilized. Results of that comparison revealed that in terms of RMSE and MPE, the QMM-calibrated models performed fairly closely to the ANFIS model, and recorded better SC-RMSE and SDE metrics.

Further evaluation of the QMM through calibration of six basic pathloss models, using measurement data for Abuja and Ibadan very clearly demonstrated that QMM-calibration of the basic models (particularly the ECC-33 models, in this case) provide excellent RMSE, MPE, MAE, and SDE results. Finally, and using a slight variation of the definition of *'cross-application'* recently introduced by Zhang et al. [35], it was shown in the paper, that when the basic models are calibrated with the average of measurements taken over several base station pathloss data, the resulting models are able, with RMSE values well-within the error bounds established by Phillips et al. [34], to predict pathloss, for individual base stations involved in the averaging.

There is still a lot of scope for further investigations into the characteristic features of the QMM, including limitations and the physical interpretations of the calibration process, as may be available from the entries into the components of the matrix expression of Eqn. (8). It is also conceivable that QMM may represent a very good candidate for some hybrid modeling process, of the type proposed in the concluding remarks of [25].

ACKNOWLEDGMENT

The authors gratefully acknowledge the access to data, generously granted by Technical Personnel of MTN and AIRTEL, both in Nigeria.

REFERENCES

[1] F. Ikegami, and S. Yoshida, "Analysis of multipath propagation structure in urban mobile radio environments". IEEE Trans. on Ant. and Propagat. AP-28(4),531-537, 1980. DOI: 10.1109/TAP.1980.1142372

[2] M. A. M. Vieira, M. E. Taylor, P. Tandon, M. Jain, R. Govidan, G. S. Sukhatme, and M. Tambe, "Mitigating multipath fading in a mobile mesh Network", Elsevier Journal on Ad-hoc Networks, 11(4), June, 2013. pp. 1510-1521. DOI: https://doi.org/10.1016/j.adhoc.2011.01.014

[3] T. K. Sarkar, Z. K. Kim, A. Medouri, and M. Salazar-Palma, "A survey of various propagation models for mobile communication". IEEE Ant and Prop Magazine. 45(3), September, 2003. pp. 51-82. DOI: 10.1109/MAP.2003.1232163

[4] A. A. Khalek, L. Al-Kanj, Z. Dawy, and G. Turkiyah, "Site placement and site selection algorithms for UMTS radio planning with quality constraints". Proceedings of IEEE 17th Int Conf on Telecom, May 2010. pp. 375-381. DOI: 10.1109/ICTEL.2010.5478775

[5] P. Calegari, F. Guidec, P. Kuonem, P. Charmaet, S. Ubeda, S. Josselin, D. Wagner, and M. Pizarosso,

"Radio network planning with combinatorial optimisation algorithms", ACTS Mobile Telecommunications Summit 96(2), 701-713, 2010. http://www-valeria.univ ubs.fr/../..storms; accessed on 18 October 2019
[6] K. Tutschku, Models and algorithms for demand-oriented planning of telecommunication systems, 1999. (PhD Thesis University of Wurzburg). Available from https://pdfs.semanticscholar.org/25aa/f7a89a6c0dd6b8439eb728c751b4671e55e5.pdf?_ga=2.172943267.1844270591.1589905218-1852863913.1589905218 Accessed May 17, 2020
[7] F. Iskander, Madgy, and Zhengqing Yun, "Propagation Prediction Models for Wireless Communication Systems", IEEE Transactions on Microwave Theory And Techniques, VOL. 50, NO. 3, MARCH 2002. pp.662-673. DOI: 10.1109/22.989951
[8] J. R. Fernandez, M. Quispe, G. Kemper, J. Samaniego, and D. Diaz, "Adjustments of log-distance path loss model for digital television in Lima" XXX Simposio Brasileiro de Telecomunicacoes, Brasilia 13-16, 2012. https://pdfs.semanticscholar.org/f892/8570f11926d0ac51b2848b0b4b7bd0684653.pdf
[9] J. Gozalvez, M. Sepulcre, and J. A. Palazon, "On the feasibility to deploy mobile industrial applications using wireless communications" Elsevier Journal of Computers in Industry, 65(8), October, 2014. pp. 1136-1146 DOI: https://doi.org/10.1016/j.compind.2014.06.004
[10] V. Erceg, L. J. Greenstein, S. Y. Tjandra, S. R. P. Parkoff, A. Gupta, B. Kulic, A. A. Julius, and R. Bianchi, "An empirically based path loss model for wireless channels in suburban environments" IEEE Journal on Selected Areas in Communications, 17(7), July, 1999. pp. 1205 -1211. DOI: 10.1109/49.778178
[11] Y. Okumura, E. Ohmori, and T. Kawano, "Field strength and its variability in VHF and UHF land mobile radio services" !6 review of the Electrical Communications Lab., Sept.-Oct. 1968, pp. 825-873.See https://www.ntt-review.jp/archive/ntttechnical.php?contents=ntr201304in1.pdf&mode=show_pdf
[12] S. Pitchaiah, "Recommendations on LMDS Radio Propagation Channel Models" IEEE 802.16.1 pc-00/44, 2000. Available from http://www.ieee802.org/16/tg1/phy/contrib/802161pc-00_44.pdf
[13] R. Mardeni and K. F. Kwan, "Optimization of Hata Propagation Prediction Model In Suburban Area in Malaysia", Progress In Electromagnetics Research C, Vol. 13, pp. 91–106, 2010.
[14] Liyth Nissirat, Mahamod Ismail, Mahdia Nisirat, "Macro-cell path loss prediction, calibration, and optimization by Lee's model for south of Amman city, Jordan at 900, and 1800 MHz", Journal of Theoretical and Applied Information Technology, Vol. 41 No.2, pp. 253-258, 2012.
[15] M. Garah, Djouane, H. Oudira, and N. Hamdiken, "Path Loss Models Optimization for Mobile Communication in Different Areas", Indonesian Journal of Electrical Engineering and Computer Science Vol. 3, No. 1, pp. 126 - 135. July 2016. DOI: 10.11591/ijeecs.v3.i1.pp126-135 201
[16] D. J. Y. Lee, and W. C. Y. Lee, "Enhanced Lee model from rough terrain sampling data aspect" 2010 IEEE 72nd Vehicular Technology Conference - Fall, Ottawa, ON, 2010, pp. 1-5, doi: 10.1109/VETECF.2010.5594119.
[17] C. Dalela, M. V. S. N. Prasad, and P. K. Dalela, "Tuning of COST-231-Hata model for radiowave propagation predictions", David C. Wyld, et al. (Eds): CCSEA, SEA, CLOUD, DKMP, CS & IT 05, pp. 255–267, 2012. DOI: 10.5121/csit.2012.2227
[18] Damosso, Eraldo, and Luis M. Correia, "COST Action 231: Digital Mobile Radio Towards Future Generation Systems" Final Report European Commission, 1999. Available from https://op.europa.eu/en/publication-detail/-/publication/f2f42003-4028-4496-af95-beaa38fd475f/language-en/format-PDFA1B
[19] Michael S. Mollel, and Michael Kisangiri, "Comparison of Empirical Propagation Path Loss Models for Mobile Communication", Computer Engineering and Intelligent Systems, Vol.5, No.9, pp. 1-10, 2014 .
[20] Sotirios P. Sotiroudis, Sotirios K. Goudos, Konstantinos A. Gotsis, Katherine Siakavara, and John N. Sahalos, "Application of a Composite Differential Evolution Algorithm in Optimal Neural Network Design for Propagation Path-Loss Prediction in Mobile Communication Systems", IEEE Antennas and Wireless Propagation Letters, VOL. 12,, pp. 364-367, 2013. DOI: 10.1109/LAW.2015.2251994
[21] Bruno J. Cavalcanti, Gustavo A. Cavalcante, "A Hybrid Path Loss Prediction Model based on Artificial Neural Networks using Empirical Models for LTE And LTE-A at 800 MHz and 2600 MHz", Journal of Microwaves, Optoelectronics and Electromagnetic Applications, Vol. 16, No. 3, pp. 708-722. DOI: http://dx.doi.org/10.1590/2179-10742017v16i3925 2017
[22] Julia O. Eichie, Onyedi D. Oyedum, Moses O. Ajewole, and Abiodun M. Aibinu "Comparative Analysis of Basic Models and Artificial Neural Network Based Model for Path Loss Prediction", Progress In Electromagnetics Research M, Vol. 61, 133–146, 2017 DOI :10.2528/PIERM17060601
[23] S. Hosseinzadeh, H. Larijani, K. Curtis, and A. Wixted, "An adaptive neuro-fuzzy propagation model for LoRaWAN", Applied System Innovation, vol. 2, no. 1. 2019. https://doi.org/10.3390/asi2010010
[24] Nasir Faruk, N. T. Surajudeen-Bakinde, Abdulkarim A. Oloyede, Segun I. Popoola, A. Abdulkarim, Lukman A. Olawoyin, and Aderemi A. Atayero, "ANFIS Model for pathloss prediction in the GSM and WCDMA bands in urban area", ELEKTRIKA, Journal of Electrical Engineering, Vol. 18(1), pp. 1-10, 2019. DOI: https://doi.org/10.11113/elektrika.v18n1.140
[25] Nasir Faruk, Segun I. Popoola, Nazmat T. Surajudeen-Bakinde, Abdulkarim A. Oloyede,

Abubakar Abdulkarim, Lukman A. Olawoyin, Maaruf Ali, Carlos T. Calafate , and Aderemi A. Atayero "Path Loss Predictions in the VHF and UHF Bands Within Urban Environments: Experimental Investigation of Empirical, Heuristics and Geospatial Models" IEEE ACCESS, Vol. 7, pp. 77293 – 77307. 2019.
DOI: 10.1109/ACCESS.2019.2921411

[26] Robson D. A. Timoteo, Daniel C. Cunha and George D. C. Cavalcanti, "A Proposal for Path Loss Prediction in Urban Environments using Support Vector Regression", Proceedings, AICT2014: The Tenth Advanced International Conference on Telecommunications, pp. 119-124. 2014.

[27] Xiaonan Zhao, Chunping Hou, and Qing Wang. "A New SVM-Based Modeling Method of Cabin Path Loss Prediction", International Journal of Antennas and Propagation, Volume 2013, Article ID 279070, 7 pages http://dx.doi.org/10.1155/2013/279070.

[28] M. Ayadi, A. Ben Zineb, and S. Tabbane, "A UHF Path Loss Model Using Learning Machine for Heterogeneous Networks", IEEE Transactions On Antennas And Propagation, Vol.65(7). pp. 3675-3683, July 2017.
DOI: 10.1109/TAP.2017.2705112

[29] MTN (Nigeria) drive test log files, private communication.

[30] Airtel (Nigeria) Drive Test log files, Private communication.

[31] G. Dahlquist, and A. Björck, (Translated by Ned Anderson) Numerical Methods, Prentice-Hall, Inc. New Jersey. 55-110, 1974.

[32] R. F. Harrington, "Matrix Methods for Field Problems", Proceedings of the IEEE, Vol. 5(2), February 1967. pp. 136-149.

[33] Nazmat T. Surajudeen-Bakinde, Nasir Faruk, Muhammed Salman, Segun Popoola, Abdulkarim Oloyede, Lukman A. Olawoyin, "On Adaptive Neuro-Fuzzy Model for Path Loss Prediction in the Vhf Band", ITU Journal: ICT Discoveries, Special Issue No. 1, Pp. 1-9, Feb, 2018.

[34] Caleb Phillips, Douglas Sicker, and Dirk Grunwald, "Bounding the Practical Error of Path Loss Models", International Journal of Antennas and Propagation, Volume 2012, Article ID 754158, 21 pages. DOI:10.1155/2012/754158

[35] Jiayi Zhang, Camillo Gentile, and Wesley Garey, "On the Cross-Application of Calibrated Pathloss Models Using Area Features", IEEE Antennas & Propagation magazine, vol. 62, no. 1, pp. 40-50, Feb. 2020.
DOI: https://doi.org/10.1109/MAP.2019.2943272